Springer

Journal of Mechanical Science and Technology 22 (2008) 1660~1667

Journal of Mechanical Science and Technology

www.springerlink.com/content/1738-494x
DOI 10.1007/s12206-008-0512-8

Development and validation of FE models of impactor for pedestrian testing

Tso-Liang Teng[1,*] and Trong-Hai Nguyen[2]

[1]*Department of Mechanical and Automation Engineering, Da-Yeh University*
[2]*Institute of Electro-Mechanical Automation Engineering, Da-Yeh University*

(Manuscript Received June 18, 2007; Revised May 3, 2008; Accepted May 19, 2008)

Abstract

Car-pedestrian accidents account for a considerable number of automobile accidents in industrialized countries. Safeguarding of pedestrians is taking on an increasingly important role in car design. Working Group 17 (WG17) of the European Enhanced Vehicle-safety Committee (EEVC) proposed four impactor models for assessing pedestrian friendliness of a vehicle. In this study, finite element models of adult headform, child headform, upper legform, and legform impactor of pedestrians were created by using LS-DYNA finite element code. The impactor structures follow the descriptions in the reports of WG17 specifications. Simulated certification tests were performed. Some materials were selected from different trademarks of the same kind of materials. The knee of the legform impactor was designed. The parameters of the springs and dampers were adjusted to satisfy the requirements. Results of simulated certification tests for the four impactors are within WG17 limit ranges. These finite element impactor models obtained herein can help evaluate the pedestrian friendliness of vehicle and guide the future development of pedestrian safety technologies.

Keywords: Pedestrian testing; Impactor FE models; EEVC WG17

1. Introduction

Traffic accidents are a common cause of mortality in modern society. According to the "*Traffic Safety Factors 2003*" of the National Highway Traffic Safety Administration (NHTSA) [1], the majority of people killed or injured in traffic accidents are drivers, followed, according to injury rates, passengers, pedestrians, motorcycle riders, and bicyclists. Vehicle safety has become the most important issue in automobile design. Hence, manufacturers now incorporate numerous safety devices and features in vehicles, including airbags, energy-absorbing steering columns, side-door beams, etc. However, all efforts to improve safety devices focus on enhancing safety features for occupants. Notably, pedestrians are the third largest category of traffic fatalities. Thus, vehicle safety should not just focus on vehicle occupant safety: protecting pedestrians is an impor-tant field in traffic safety.

Over the past few years, most attempts to reduce pedestrian fatalities and injuries have focused solely on isolation techniques, such as pedestrian bridges, public education, and traffic regulations [2-4]. Developing pedestrian-friendly vehicles is one solution for reducing the pedestrian fatality rate. Manufacturers currently attempt to produce enormous benefits for vehicle occupants enhancing pedestrian safety when impacting a vehicle with compliant bumpers, dynamically raised bonnets, and windscreen airbags [5-7]. To assess the degree of pedestrian protection of a vehicle, it is necessary to develop an efficient evaluation and analysis methodology to examine vehicles for pedestrian protection. The EEVC, IHRA and Global Technical Regulation (GTR) have developed pedestrian subsystem test methods that assess vehicle capabilities to protect pedestrian during accidents. In

*Corresponding author. Tel.: +886 4 841 1221
E-mail address: tlteng@mail.dyu.edu.tw

the late 1980s, the EEVC began developing a set of standards that can minimize serious injury to pedestrians when impacted by a vehicle traveling at 40 km/h [8]. The EEVC Working Group 17 (WG17) established a series of component tests representing the three most important mechanisms of injury: head, upper leg, and lower leg. The EEVC WG17 proposed this method for assessing whether a vehicle was pedestrian friendly. The WG17 tests comprise four models of pedestrian impactors that typically impact with four corresponding areas on a vehicle. Fig. 1 presents the pedestrian protection concept proposed by WG17. The European Union has utilized these pedestrian safety regulations for vehicle tests. These WG17 regulations will be completed and applied to vehicle manufacturing in Europe.

Recently, developments in computer technology have allowed applied mathematicians, engineers, and scientists to solve previously intractable problems. Simulation tools for predicting occupant or pedestrian kinematics and injury criteria include MADYMO, Pam Crash, and LS-DYNA3D [9-12]. Numerical simulations are valuable design tools for automotive engineers. To optimize pedestrian protection in various situations, finite element modeling can be employed to evaluate vehicle-pedestrian impact. The versatility and low repeating cost of the finite element method helps designers to perform many more tests for pedestrian safety. To evaluate pedestrian protection, this study adopts WG17 regulations of certification tests for the pedestrian impactor models. The method used to build finite element impactor models with LS-DYNA3D is described in detail. Simulated certification tests were performed. Simulation results were then presented and analyzed. These finite element impactor models can be employed to examine the ability of vehicles to injure pedestrians and their role in future development of pedestrian safety technologies

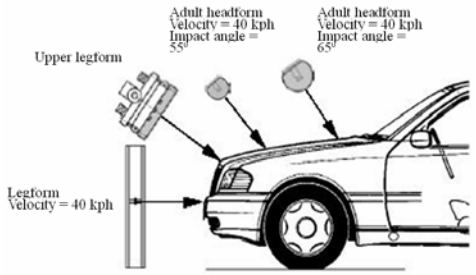

Fig. 1. Pedestrian protection concept of WG17 [13].

2. WG17 report for certification tests

Sub-system WG17 impactor tests cover most possible impact locations on the vehicle front: hitting the bonnet with free-flying head forms; the leading edge of the bonnet impacting a proximal lower limb; and the bumper contacting a leg form containing a deformable knee joint. These impactors have force, displacement, and acceleration sensors. Sensor data is interpreted relative to biomechanical tolerance levels of the human head and lower limbs.

2.1 Headform certification tests

The headform impactors were employed in the headform to bonnet top tests (Fig. 1). Fig. 2 shows the certification test configurations. The headforms are hung with 2 m of rope. A 3-kg aluminium impactor with initial velocity of 7 m/s impacts the headform impactor. The suspension angle can be changed from 25-90°. Acceleration is measured at the center of gravity of the headform. For the child and adult headforms, the resulting peak acceleration must fall between 405-495g for adult headforms and 337.5-412.4 g for child headforms.

2.2 Upper legform certification test

The upper legform is utilized in the upper legform-to-bonnet leading-edge tests (Fig. 1). Fig. 3 shows the configuration of the certification test. A 12-kg upper legform set at an initial velocity of 7.1 m/s impacts a 3-kg steel pendulum hung on a 2 m length rope. Peak axial force on the transducers must be greater than

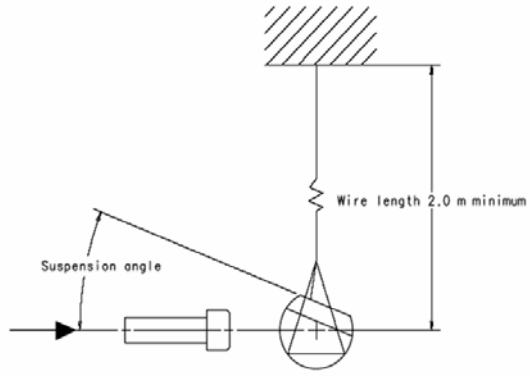

Fig. 2. Headform certification test [13].

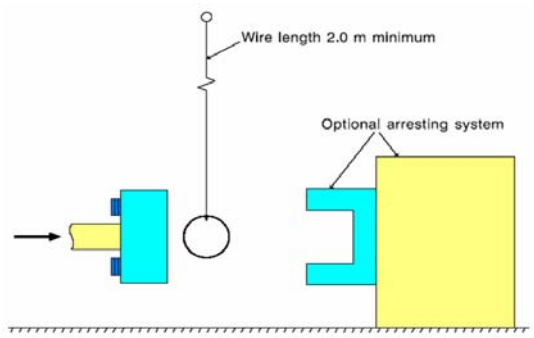

Fig. 3. Certification test of the upper legform [13].

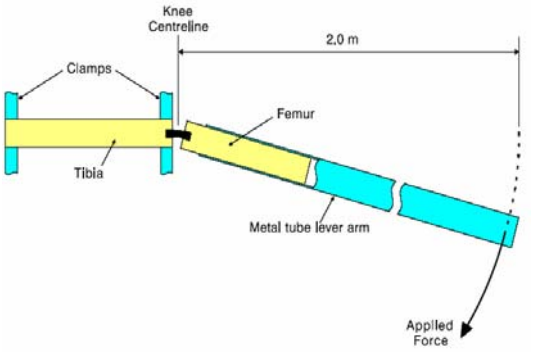

Fig. 4. Static bending certification test of the legform[13].

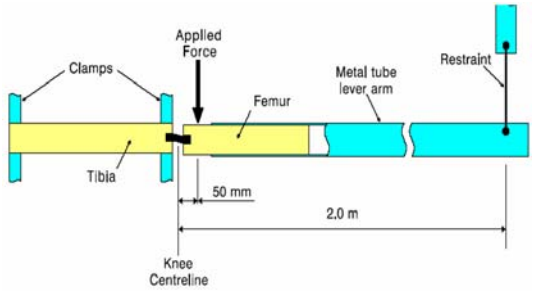

Fig. 5. Static shearing certification test of the legform[13].

1.20 kN and less than 1.55 kN. The peak bending moment (on center position) must be greater than 190 Nm and less than 250 Nm. Peak bending moment (at the outer position) must be greater than 160 Nm and less than 220 Nm. The differences between peak values of the axial force and bending moment at different positions are also considered.

2.3 Legform certification tests

The legform is utilized in the legform-to-bumper test (Fig. 1). Before this test is conducted, the legform must satisfy the requirements of one dynamic and two

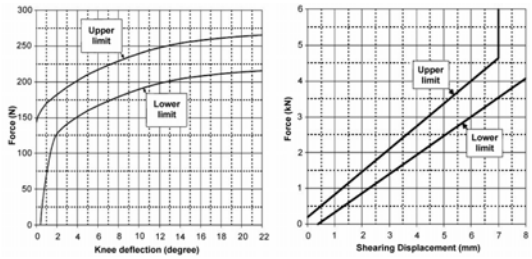

(a) (b)

Fig. 6. The requirements of static certification tests of the legform[13].

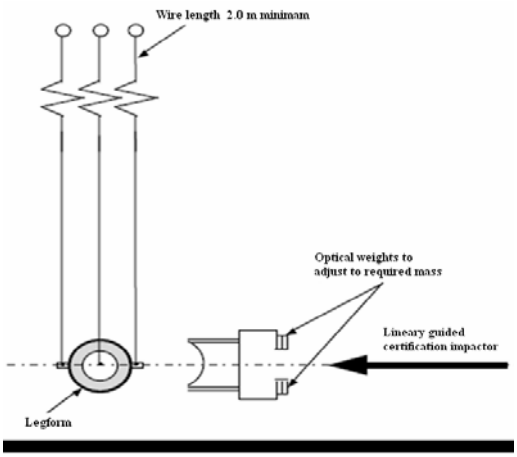

Fig. 7. Dynamic certification test of the legform[13].

static certification tests. Figs. 4 and 5 present the configurations of the static bending and the static shearing certification tests for the legform. The first test assesses the bending ability of the legform and the second test checks the knee's shearing ability. During simulation or tests, the time interval applied to the load on the legform must be considered. That is, the energy taken to generate 15° of bending must be 100 J.

Figs. 6(a) and 6(b) list the requirements of the two tests. The force vs. angle of static bending test must be between upper and lower limits, as specified in Fig. 6(a). Fig. 6(b) shows the requirement of the force vs. displacement curve of the static shearing certification test. Fig. 7 illustrates the configuration of the dynamic certification test. The 12.4-kg upper legform set at an initial velocity of 7.5 m/s impacts a pendulum hung on a 2-m-long rope. The maximum upper tibial acceleration is 120-250 g. Maximum bending angle is from 6.2-8.2°. Maximum shear displacement is 3.5-6.0 mm.

3. FE Models of pedestrian impactor

3.1 Headform impactors

3.1.1 Headform impactor description

The child and adult headform impactors have aluminum cores covered with 10.0 ± 0.5 mm and 13.9 ± 0.5 mm vinyl skins, respectively. Total is 2.5 ± 0.1 kg for the child and 4.8 ± 0.1 kg for the adult headform impactor. Accelerometers are mounted at the sphere center for both headform impactors (Figs. 8 and 9).

3.1.2 Finite element models

Fig. 10 shows the finite element models of the child and adult headform impactors. The vinyl skin is modeled with viscoelastic material, and steel core with elastic material. All impactor parts use solid elements. The adult impactor model consists of 3,713 nodes and 13,783 solid elements. The child impactor model consists of 2,021 nodes and 7,032 solid elements.

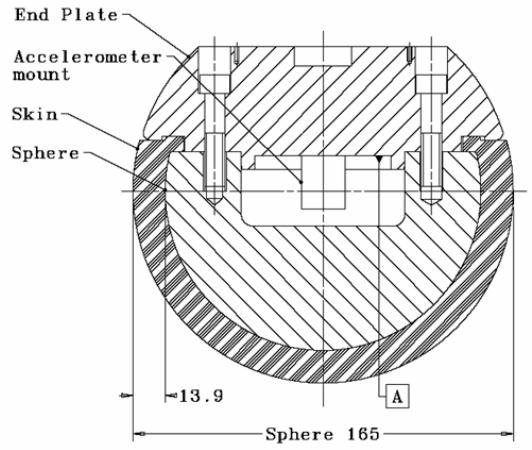

Fig. 8. Adult headform impactor (dimension in mm)[13].

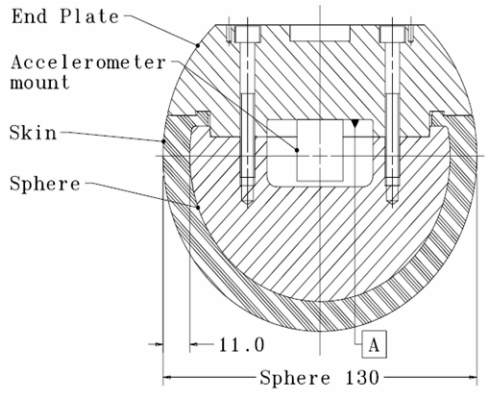

Fig. 9. Child headform impactor (dimension in mm)[13].

3.2 Upper legform impactor

3.2.1 Upper legform impactor descriptions

The pedestrian femur is modeled with a steel cylinder. The flesh is modeled with sheets of CF-45 foam 25 mm thick. The skin is a layer of 1.5-mm-thick fiber-reinforced rubber (Fig. 11). The cylinder is connected with the rear parts by two transducers at its ends. Extra weights are used to adjust the mass of the upper legform at different impact speeds. The torque-limiting joint is employed to attach the upper legform to the propulsion system. Three strain gauges are located at the non-impact side of the cylinder to measure the bending moments at specific positions. Axial forces are measured with transducers.

3.2.2 Finite element models

Fig. 12 illustrates the finite element model of upper legform. The foam CF-45 is modeled with a low-

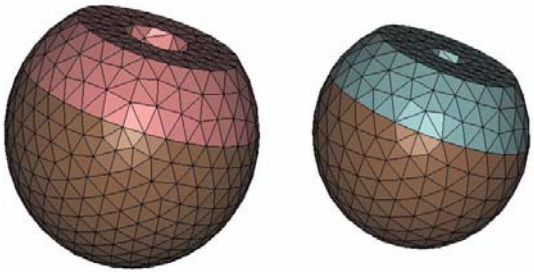

Fig. 10. Finite element models of adult and child headform.

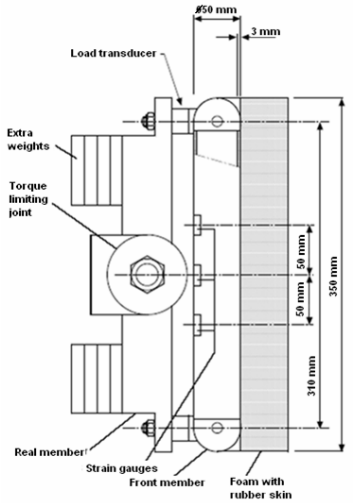

Fig. 11. Upper legform impactor[13].

density foam material. Fig. 13 presents the stress-train curve for foam CF-45 material. The rubber skin consists of an elastic material. The cylinder consists of an elastic material. The rear parts are modelled with a rigid material. This model consists of 5,823 nodes, 2 beam elements, 1,622 shell elements, and 2,388 solid elements. The cylinder is modeled by using shell elements. The caps are spotwelded to the cylinder. Spotweld connections are distributed evenly throughout the cylinder's circumference. The two transducers are modeled with two beams with corresponding parameters that fit with the joints at their two ends. Each transducer is fixed to the rear part by bolt connection and to the cylinder by a revolute joint. Thus, to simulate the transducer, the beams must be stable in the axial y direction, cannot be bent so much about x axis, cannot be twisted much about z axis, and can be bent about the y axis with a little resistance. Consequently, the beams must have a large cross-sectional area, a large moment of inertia about the x-axis, a large polar moment of inertia about z-axis, and a small moment of inertia about y axis. Because the cylinder is used to measure the bending moment and the transducers have revolute joints, the way to represent the transducers by the beams would affect the results. To avoid the bending of the transducers in the plane perpendicular to the symmetric plane, the moment of inertia about the cylinder axis should be sufficiently large. To avoid transducer twisting, the polar inertia should not be too small. To model revolute joints, the transducers can be bent slightly in the symmetric plane. Thus, the moment of inertia about the axis perpendicular to the symmetric plane should be small. All rear parts are modeled by using rigid materials and fixed together with rigid connections.

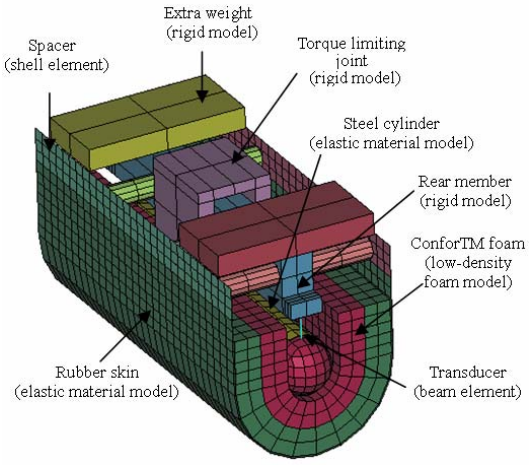

Fig. 12. Finite element model of upper legform.

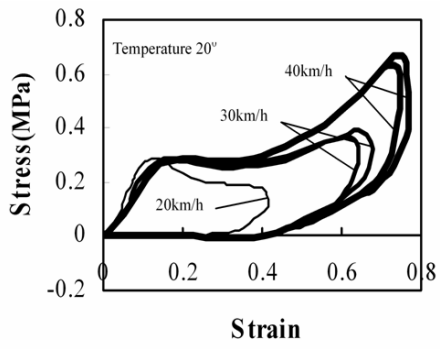

Fig. 13. The stress-strain curve of CF-45 foam material[9].

3.3 Legform impactor

3.3.1 Legform impactor descriptions

The human femur and tibia are modeled with two steel cylinders, both 70 mm in diameter. The two cylinders are connected with a joint, representing a knee with two degrees of freedom (Fig. 14). The knee can bend and shear. The bending angle and shear displacement are measured at the knee center. The legform is covered with 25 mm of CF-45 foam and 6 mm of neoprene represents flesh and skin, respec-

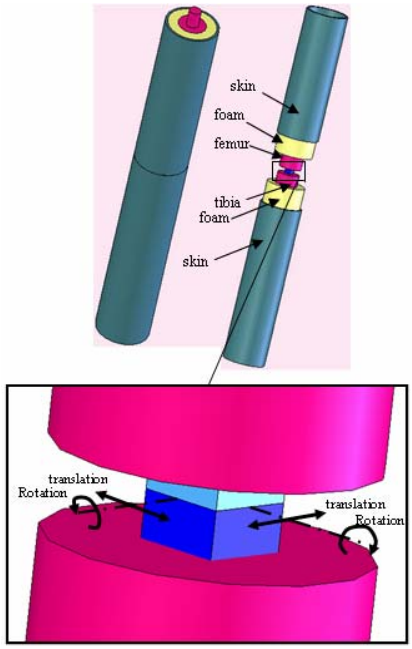

Fig. 14. Legform impactor.

tively. Legform acceleration is measured on the non-impact side, 66 mm under the knee. The bending angle and shear displacement are measured at the knee.

3.3.2 Finite element models

This model consists of 4,820 nodes, 10 beams, 1,210 shell elements, and 3,324 solid elements (Fig. 15). The tibia and femur utilize shell elements and a rigid material to represent the cylinders and steel material. The flesh is constructed of solid elements and a low-density foam model to represent CF-45 material. The foam used is the same as that on the upper legform. The skin consists of solid elements and an elastic material model to represent neoprene material.

The knee is represented with 16 rotational/translational springs and dampers (Fig. 16). One and four beams are connected rigidly to the lower and upper knee, respectively. Then, each spring or damper is connected to one beam on the upper knee and one on

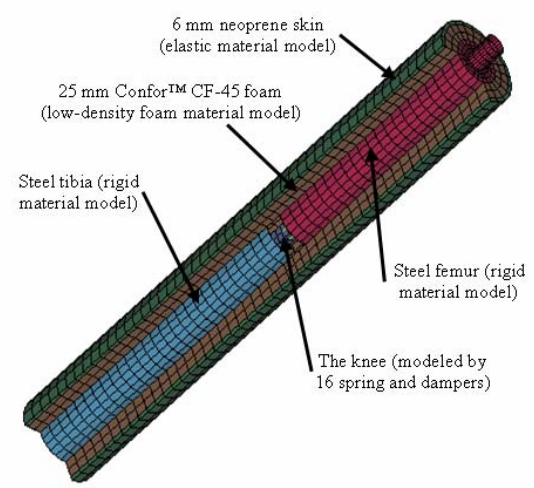

Fig. 15. Finite element model of legform.

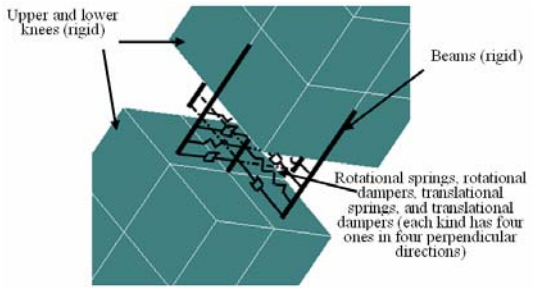

Fig. 16. The knee of the legform impactor.

4. Certification test simulations of FE models

4.1 Headform impactor certification test simulations

Each headform was certified by three simulations at three different suspension angles. The acceleration peak of the child headform in the certification test simulation fit within limits and considerably close to the upper limit (Fig. 17). Analytical results of three simulations were quite similar. Acceleration of the adult headform in the certification test simulation fell within the acceptable range (Fig. 18). Analytical results of the three simulations were extremely similar. The headform impact models, thus, were valid according to EEVC WG17 specifications (Figs. 17 and 18).

4.2 Upper legform impactor certification test simulations

Fig. 19 presents the simulation result for the bending moment at the cylinder's center position in the certification test. The curve peak fell within limits and was comparable with the bending moment of the cylinder's outer position (Fig. 20). The axial force measured at the transducers also satisfied require

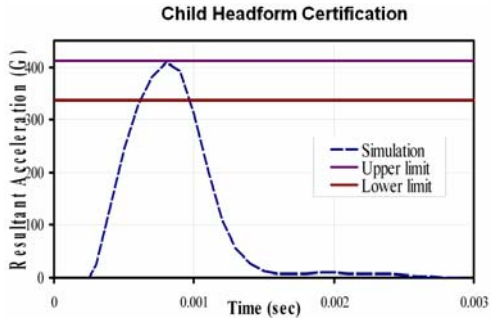

Fig. 17. The acceleration time history of the child headform impactor in certification test simulation.

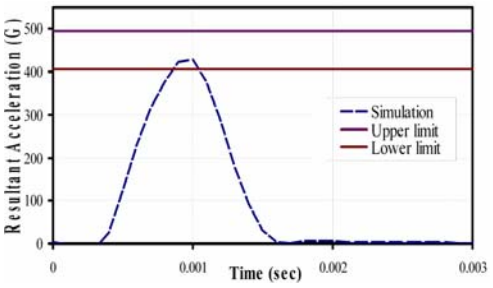

Fig. 18. The acceleration time history of the adult headform impactor in certification test simulation.

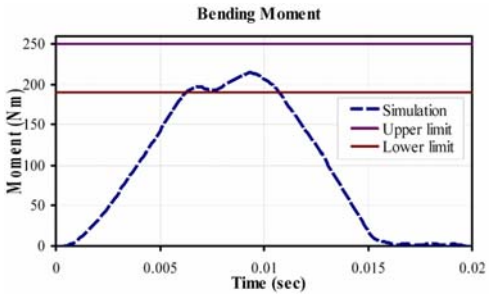

Fig. 19. The bending moment time history at the center position of upper legform impactor in certification test simulation.

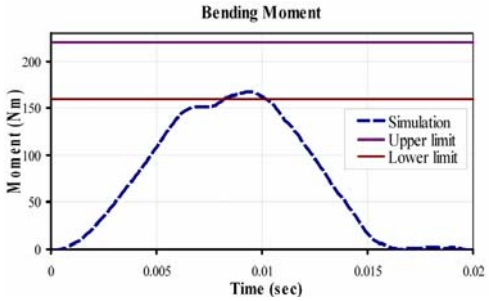

Fig. 20. The bending moment time history at the outer position of upper legform impactor in certification test simulation.

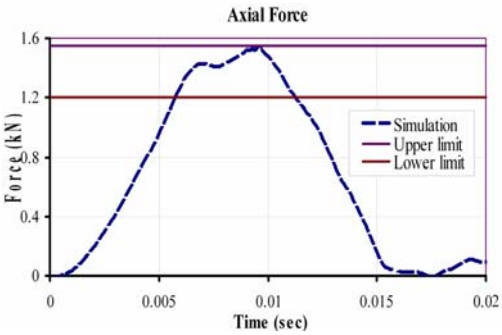

Fig. 21. The axial force time history at the transducer of upper legform impactor in certification test simulation.

ments (Fig. 21). The peak value was significantly close to the upper limit. A minor difference exists between the axial forces on the top and bottom transducers. Simulation results indicate that the upper legform impact model conforms to EEVC WG17 speci-fications (Figs. 19-21).

4.3 Legform impactor certification test simulations

First, the first static test simulation for the legform to examine the force vs. bending angle was performed. During this simulation, rotational spring properties were adjusted to conform to static test requirements (Fig. 22). Then, the second static test simulation for

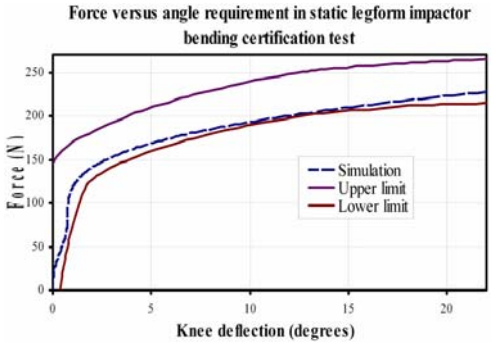

Fig. 22. The force versus bending angle of the legform impactor in certification test simulation.

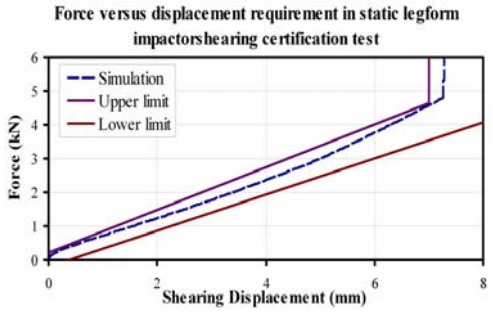

Fig. 23. The force versus shearing displacement of the legform impactor in certification test simulation.

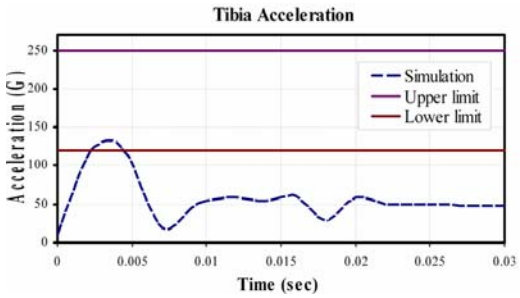

Fig. 24. The acceleration time history of the tibia in certification test simulation.

the legform to examine the force vs. shearing displacement was performed. In this simulation, translational spring properties were adjusted to meet the requirements (Fig. 23). The dynamic test simulation was then performed. During this simulation, rotational and translational dampers were adjusted to meet the requirements (Figs. 24-26). Lastly, static test simulations were performed to check the knee's static properties. This procedure was repeated until all requirements of certification test are satisfied. Experimental results from the two static and dynamic test simulations are show in Figs. 22-26, so the legform

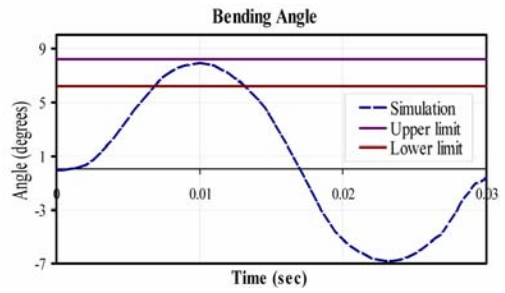

Fig. 25. The bending angle time history of the knee in certification test simulation,

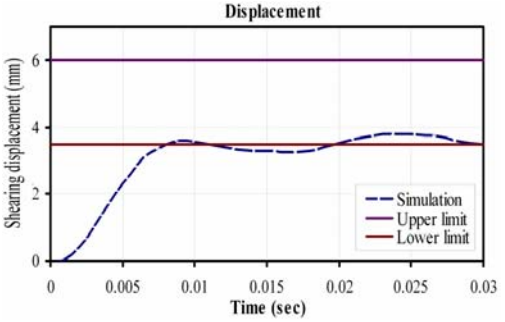

Fig. 26. The shearing displacement time history of the knee in certification test simulation.

impact model conforms to EEVC WG17 specifications.

5. Conclusions

Simulation models for the child headform, adult headform, upper legform, and legform impactor were developed by using LS-DYNA3D. These models were based on EEVC WG17 specifications. Realistic validation tests were performed in order to get a basis for the numerical validation procedure. Simulations also satisfy all WG17 requirements for certification tests. Two headform impactors, an upper legform and a legform impactor are available. These reasonable, well validated numerical impactor models can be used to predict front vehicle behavior to determine the pedestrian friendliness of a vehicle, support virtual design process and provide direction for future development of pedestrian safety technologies.

References

[1] Traffic Safety Facts 2003, National Highway Traffic Safety Administration, USA, (2004).

[2] O. M. J. Carsten, D. J. Sherborne and J. A. Rothengatter, Intelligent Traffic Signals for Pedestrians: Evaluation of Trials in Three Countries**,** Transportation Research Part C: Emerging Technologies, 6 (1998) 213-229.

[3] T. Ross, A. J. May and P. J. Grimsley, Using Traffic Light Information as Navigational Cues: Implications For Navigation System Design, Transportation Research Part F: Traffic Psychology and Behaviour, 7 (2004) 119-134.

[4] J. R. Sayer and M. Lynn Mefford, High Visibility Safety Apparel and Nighttime Conspicuity of Pedestrians in Work Zones, Journal of Safety Research, 35 (2004) 537-546.

[5] T. Maki and T. Asai, Development of Pedestrian Protection Technologies for ASV, JSAE Review, 23 (2002) 353-356.

[6] A. Zanella, F. Butera, E. Gobetto and C. Ricerche, Smart Bumper for Pedestrian Protection, Smart Materials Bulletin, 2002 (7) (2002) 7-9.

[7] Y. H. Han and Y. W. Lee, Development of a Vehicle Structure with Enhanced Pedestrian Safety, SAE Word Congress 2003, Detroit, (2003) No.2003-01-1232.

[8] M. P. Paine and C. G. Coxon, Assessment of Pedestrian Protection Afforded by Vehicles in Australia, Impact Biomechanics & Neck Injury 2000, Sydney (2000).

[9] A. Konosu, H. Ishikawa and R. Kant, Development of Computer Simulation Models for Pedestrian Subsystem Impact Tests, JSAE Review, 21 (2000) 109-115.

[10] A. Deb and T. Ali, A Lumped Parameter-based Approach for Simulation of Automotive Headform Impact with Countermeasures, International Journal of Impact Engineering, 30 (2004) 521-539.

[11] H. Ishikawa, J. Kajzer, K. Ono and M. Sakurai, Simulation of Car Impact to Pedestrian Lower Extremity: Influence of Different Car-front Shapes and Dummy Parameters on Test Results, Accident Analysis & Prevention, 26 (1994) 231-242.

[12] P. Niederer, An Experimental and Theoretical Simulation Study of Vehicle-pedestrian Accidents, Journal of Biomechanics, 18 (1985) 555.

[13] European Enhanced Vehicle Safety Committee (EEVC) Working Group 17, Improved Test Methods to Evaluate Pedestrian Protection Afforded by Passenger Cars, (2002).